

Working Principle of the Hollow-Anode Plasma Source

André Anders and Simone Anders

Lawrence Berkeley National Laboratory,
University of California, Berkeley, CA 94720

Abstract

The hollow-anode discharge is a special form of glow discharge. It is shown that a drastically reduced anode area is responsible for a positive anode voltage drop of 30-40 V and an increased anode sheath thickness. This leads to an ignition of a relatively dense plasma in front of the anode hole. Langmuir probe measurements inside a specially designed hollow anode plasma source give an electron density and temperature of $n_e = 10^9 - 10^{11} \text{ cm}^{-3}$ and $T_e = 1 - 3 \text{ eV}$, respectively (nitrogen, current 100 mA, flow rate 5-50 scc/min). Driven by a pressure gradient, the "anode" plasma is blown through the anode hole and forms a bright plasma jet streaming with supersonic velocity (Mach number 1.2). The plasma stream can be used, for instance, in plasma-assisted deposition of thin films.

Introduction

Sources of flowing plasma ("downstream plasma sources") and low-energy ion beam sources are used for plasma-assisted thin film deposition or molecular beam epitaxy (MBE) of thin films, among others applications. Today, almost all MBE plasma and ion beam sources are based on plasma production by microwaves in a magnetic field (ECR plasma sources: resonance of microwave and electron cyclotron frequency), by radio frequency (RF) excitation and ionization, or by using a low-voltage discharge (in a magnetic field) sustained by a heated tungsten filament (Kaufman ion sources).

A different and simple form of discharge was invented by Miljevic [1, 2]. He modified a glow discharge using a concave cathode and a small hollow anode. A discharge gas is fed through an opening in the cathode and leaves the discharge chamber through the hollow anode as a flow of plasma, driven by the pressure gradient (Fig. 1). The brightest part of the discharge is located in and around the hollow anode, which led to the name hollow-anode discharge [1]. Miljevic [3] concludes: "Due to beam-like properties of the electron stream and focusing of the concave cathode, the high density of the high-energy electrons in the hollow anode is provided. In this way the probability for collisions of electrons with atoms, passing through the hollow anode, is increased and the intensive ionization and excitation of the atoms is observed." This interpretation was kept although Miljevic himself showed [4] that the hollow-anode discharge works fine with a flat cathode, too. There is obviously a need for a better understanding of the working principle of this kind of plasma source.

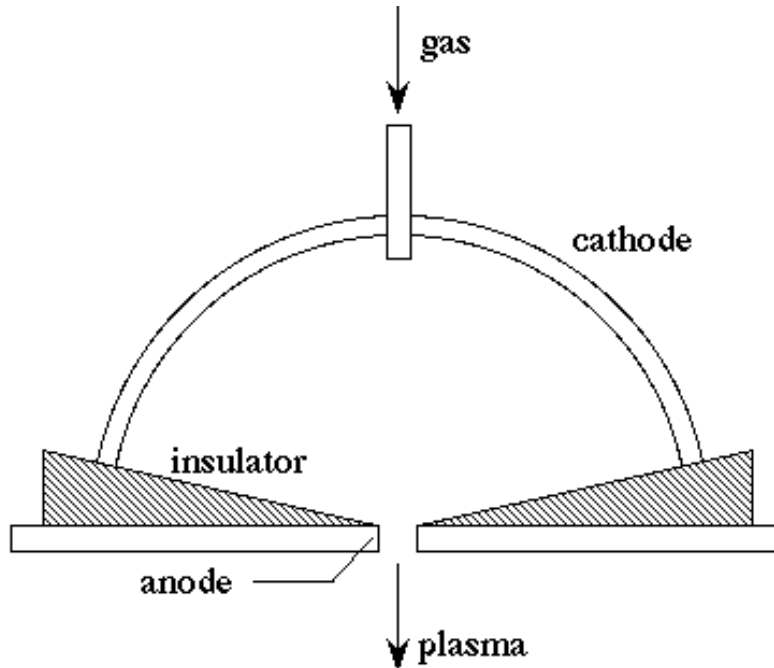


Fig. 1 Basic design of a hollow-anode discharge (after Miljevic [2]).

Experiments

Considering the differences between an ordinary glow discharge at low gas pressure and Miljevic' hollow-anode discharge, it seems quite obvious that the reduced anode area is important for the observed hollow-anode effect. In order to investigate this we have built a number of hollow-anode plasma sources. One of them is shown in Fig. 2. The discharge tube had a cross section of 40 cm^2 ; the area equals the anode area if insulating barrier is removed. The cathode-anode distance was 10 cm, determined by the length of the glass insulator between them. We have chosen glass because it allows direct observation of the anode region. The hole of the anode and insulating anode barrier (alumina, thickness 0.5 mm) had a diameter of 2 mm, i.e., its cross section was only about 0.08% of the anode area with the barrier removed. Nitrogen gas was fed through a hole (diameter 5 mm) in the cathode at a flow rate in the range 1-100 scc/min; the pressure inside the source was about 40 Pa (300 mTorr) and outside the source three orders of magnitude lower, pumped by a cryogenic vacuum pump. A voltage of in the range from -600 V to -1 kV was applied to the cathode via a load resistor of $1 \text{ k}\Omega$, while the anode was at ground potential. A glow discharge ignited when the cathode-anode voltage surpassed 500 V. The self-sustained cathode-anode voltage (during operation) was in the range of 450 - 800 V with a discharge current in the range of 20-200 mA, both depending on the supplied voltage and flow rate.

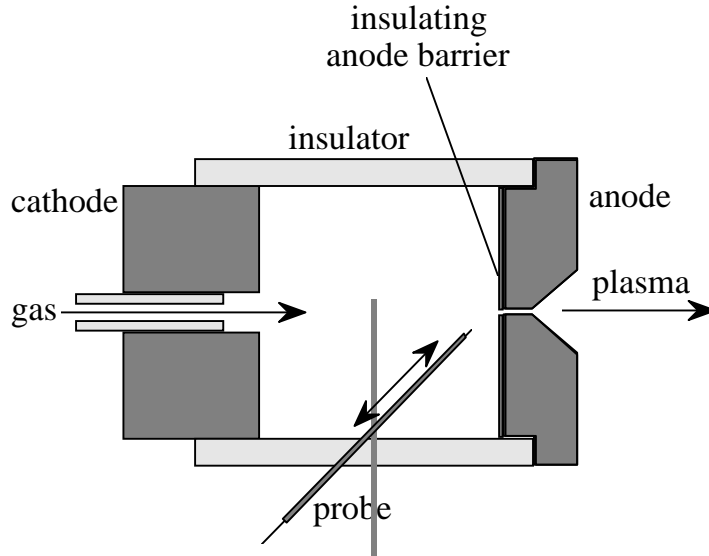


Fig. 2 Hollow-anode plasma source with probe.

The plasma source was equipped with a movable Langmuir probe which could approach the center of the hollow anode opening under an angle of 45° . The cylindrical probe (stainless steel, radius $150\ \mu\text{m}$, length $1\ \text{mm}$) was shielded by a ceramic insulator. A sawtooth-shaped probe voltage was provided by a function generator (sweep time $0.1\ \text{s}$) and coupled to an operational amplifier (max. amplitude $500\ \text{V}$). Probe characteristics was measured using a 4-channel digitizing oscilloscope. The plasma parameters (density, electron temperature, floating and plasma potential) have been determined from the probe characteristics using well-known procedures (see, for instance [5], and explanations given below). An additional flat Langmuir probe (diameter $2.5\ \text{cm}$) or a large flat ion collector (diameter $12\ \text{cm}$) were used outside (downstream) the plasma source in order to measure the output and properties of the plasma leaving the source.

First we used the source without the insulating barrier (large anode area). The nitrogen flow leaving the source through the anode hole was almost invisible, indicating a very low degree of ionization. Indeed, we were not able to detect any ion saturation current using the ion collector which was located $8\ \text{cm}$ downstream the anode hole; the ion current drawn was less than $0.1\ \mu\text{A}$. Since there was no bright plasma at the anode hole we concluded that this is an ordinary glow discharge with negligible plasma flow. Using the movable Langmuir probe inside the source we found that the anode voltage drop is, as found by others, about $15\ \text{V}$, i.e. approximately equal to the ionization potential of nitrogen. The sheath thickness was smaller than $2\ \text{mm}$ and could therefore not very well mapped.

In the next experiment we used the same setup and parameters but covered the anode to block all of its surface except its hollow part. While most of the discharge appeared similar to the usual glow discharge, a distinct, very bright plasma region at the anode was observed, and the outflowing nitrogen was clearly ionized and excited. The built-in Langmuir probe was used to determine the plasma parameters as a function of distance, d , to the anode hole center (hole center in the plane of the discharge-facing side of the ceramic anode cover). Figure 3 shows the plasma potential as a function of d for two different flow rates. Comparison with the data mentioned above shows that (i) the anode fall is significantly greater than without insulating anode barrier and (ii), the anode

sheath thickness is increased. The internal gas pressure (inside the plasma source), the discharge current, anode-cathode voltage and all plasma parameters (density, electron temperature, plasma potential) depend on the flow rate. Keeping the supply voltage constant, we observe a maximum in the discharge current (180 mA), the anode drop (about 40 V), plasma brightness, and plasma output (Fig. 4) at a flow rate of about 50 scc/min. Note that the anode drop has a maximum although the cathode-anode voltage has a minimum as a consequence of the maximum voltage drop across the load resistor at maximum current.

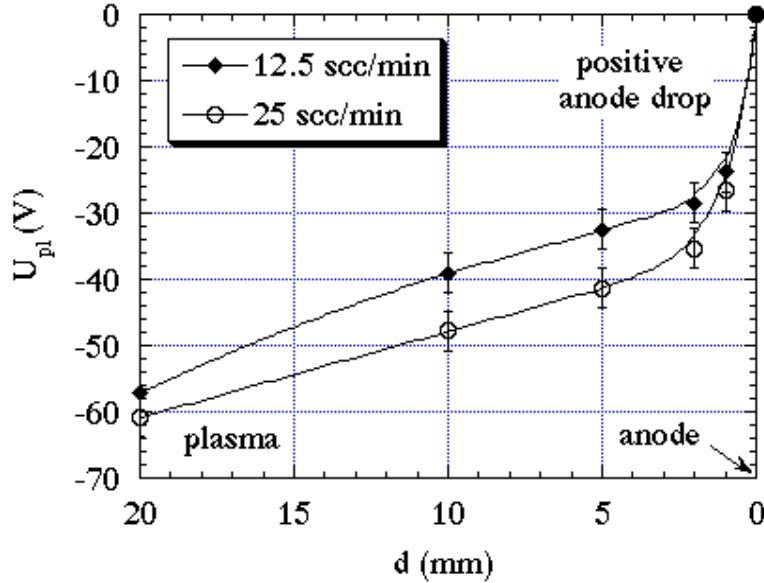


Fig. 3 Plasma potential as function of distance to the anode hole center.

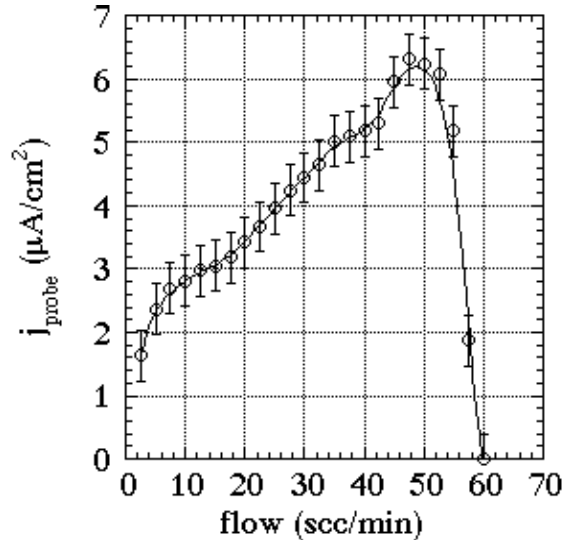


Fig. 4 Output of the plasma source measured by a Langmuir probe (ion saturation current) as a function of the nitrogen gas flow; the probe was located 8 cm downstream from plasma source, discharge current was 30-100 mA depending on flow rate.

The electron temperature was determined from the slope of the ion-current-corrected electron characteristics [5],

$$T_e = \frac{e}{k} \left[d \left(\ln \frac{I_e}{I_{e0}} \right) / dU \right]^{-1} \quad (1)$$

where I_e is the electron current and I_{e0} a normalization current, U is the probe potential, and e and k are the elementary charge and the Boltzmann constant, respectively. The logarithmically presented data can be fitted by a straight line, indicating that deviations from a Maxwell distribution are small. Results of electron temperature measurements are shown in Fig. 5.

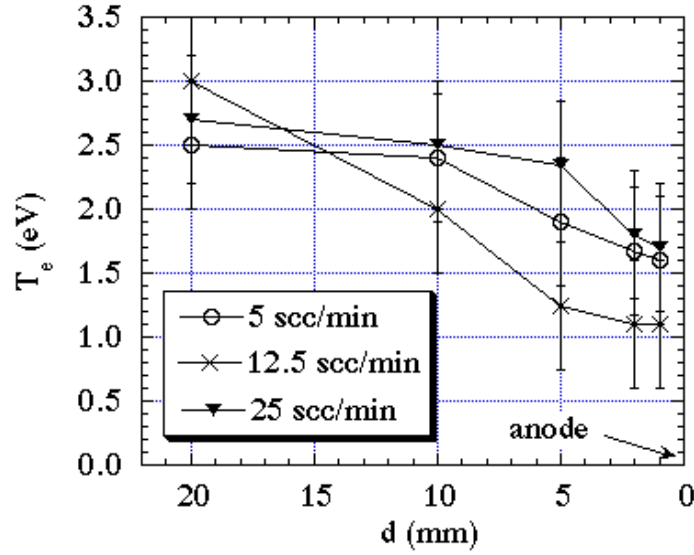


Fig. 5 Spatial distribution of the electron temperature inside the hollow anode plasma source for three different flow rates (5, 12.5, 25 scc/min) at constant supply voltage (600 V); d is the distance of probe tip to the center of the anode hole; cathode-anode voltage and discharge current was 578 V, 512 V, 460 V, and 12 mA, 44 mA, 69 mA, respectively.

The plasma potential was determined using two methods. With the electron temperature known, the formula [5]

$$U_{fl} = -\frac{kT_e}{e} \ln \left(\sqrt{\frac{m_i}{m_e}} \right) \approx -5.4 kT_e \quad (2)$$

was used to derive the plasma potential from the measured floating potential; m_i/m_e is the mass ratio of ions and electrons, and the factor 5.4 is valid for molecular nitrogen ions. The second method is to identify the probe voltage at which the electron branch of the characteristic exhibits a slight kink. Both methods are in agreement within the error range of about ± 5 Volts. Results are shown in Fig. 3.

The electron density inside the source was determined using the theory of cylindrical probes with extended sheath [5]

$$n_e = \frac{\pi I_e}{e A_p} \left(\frac{m_e}{2kT_e} \right)^{1/2} \left(1 + \frac{eU}{kT_e} \right)^{-1/2} \quad (3)$$

where I_e is the electron current to the probe (probe current correct for ion current), A_p is the probe area, and the probe potential U is here with respect to the plasma potential (not ground potential). For sufficiently large probe potentials, $eU \gg kT_e$, one obtains a temperature-independent way of determining the electron density:

$$n_e = \frac{\pi I_e}{e A_p} \left(\frac{m_e}{2eU} \right)^{1/2} \quad (4)$$

The results are shown in Fig. 6. Although the accuracy is not very great (in particular for the data point at $d = 1$ mm), our measurements indicate that the increase in density is overexponential when approaching the anode hole.

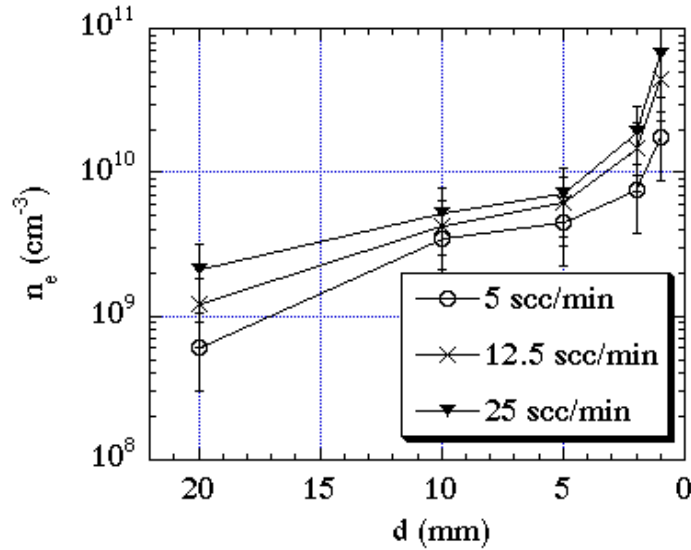


Fig. 6 Electron density measured inside a hollow anode plasma source (same conditions as in Fig. 5).

In order to confirm the important role of the anode area and anode drop we replaced the “hollow” anode (anode with hole) by a plane anode without hole. Of course, there was no gas flow in this experiment but the discharge operated at static pressure. The pressure in the vacuum chamber was equal to the pressure inside source since the gas feeding hole in the cathode was open. We used the same insulating barrier to cover most of the anode except a central area of about 3 mm^2 . The pressure was slowly increased, and the discharge ignited at 17 Pa (130 mTorr). A bright “plasma ball” appeared at the anode, very similar to the plasma previously formed at the anode hole. The anode plasma

was brightest at a pressure of 43 Pa (325 mTorr). Probe measurements show similar plasma parameters as in the case of the hollow anode; the anode voltage drop was slightly greater. The anodic "plasma ball" was not present when the insulating barrier was removed, and a usual glow discharge was observed.

Finally we determined the flow velocity of the weakly ionized plasma leaving the anode hole. From the pressure ratio (inside/outside) and the flow rate one can easily estimate that the flow velocity should be of order 500 m/s, i.e. surpassing sound speed. The anode hole acts like a nozzle, and such high speed is not surprising. We used Mach's cone method to determine the local Mach number 2 cm downstream the anode hole (Fig. 7). The streaming velocity, v , can be found by measuring the angle α and using the relation

$$M = \frac{v}{c} = 1/\sin \alpha \quad (5)$$

where c is the sound speed. The angle was found $\alpha = 60^\circ \pm 3^\circ$ when the flow rate was smaller than 30 scc/min. At greater flow rates, the plasma jet became very bright and diffuse, and no clear angle could be identified. The measured angle results in $M = 1.15 \pm 0.04$. The sound speed depends on the gas temperature, T_g , according to

$$c = \sqrt{\kappa R T_g / \mu_g} \quad (6)$$

where κ is the ration of specific heats, R is the universal gas constant, and μ_g is the molar mass of the gas. For nitrogen we obtain $c = 350$ m/s at room temperature and about 390 m/s at $T_g = 100^\circ\text{C}$. The flow speed is therefore $v = 400 - 460$ m/s, in good agreement with initial estimates.

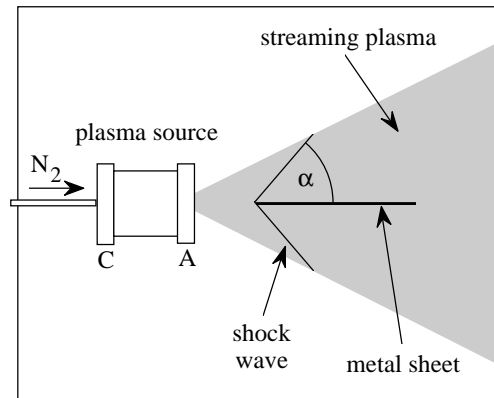


Fig. 7 Measurement of the local Mach number using Mach's cone method.

The ion density outside the source is an important parameter for thin film synthesis. Since the flow is supersonic we use the flow speed (rather than the Bohm velocity) and the measured ion saturation current (Fig. 4) to determine the ion density:

$$n_i \approx j_i / e v \quad (7)$$

We obtain values in the range $n_i = 2 - 8 \times 10^8 \text{ cm}^{-3}$, depending similarly on the flow rate as the ion saturation current (Fig. 4). This corresponds to a particle flow density of $1 - 4 \times 10^{11} \text{ ions / cm}^2 \text{ s}$ in 8 cm distance from the plasma source. Note that the particle flow density could be much greater by increasing the plasma source power and operating with an optimum flow rate at maximum discharge current.

From the electron or ion density on the one hand and the pressure on the other we can determine the degree of ionization inside and outside the plasma source. In both areas we obtain values in the range $10^{-4} - 10^{-6}$ with the highest values at the optimum flow rate of about 50 scc/min and maximum current of about 100 mA. It is not surprising that the degree of ionization outside the source is not significantly smaller than near the much denser anode plasma because it is known that an expanding low-pressure plasma is in thermal and thermodynamic non-equilibrium.

Discussion

A comparison of the hollow-anode discharge with an ordinary glow discharge shows that the key difference is not the cathode shape but the small anode area obtained by shielding most of the anode by an insulating barrier. It has been known since the fundamental work of Langmuir and Smith-Mott [6] that an electric sheath exists around an electrode, the thickness and potential drop of which can be determined by balance equations. Sheath thickness, sign of the anode potential drop and space charge are determined by the condition that the current at the anode surface must equal the discharge current (which is, in turn, determined by the outer circuit and the discharge itself). The anode acts usually only as a collector of electrons and repels ions; thus a layer of electrons is in the vicinity of the anode surface. This layer represents a sheath of negative space charge and is, as a consequence of the Poisson equation, associated with a positive anode fall (Fig. 8, curve (a)) which is typically of order the ionization potential of the gas [7, 8]. This is for nitrogen molecules 15.5 eV [9]. It is known that a reduction of the anode size leads to an increase of the anode fall (see review by Francis [7], p.146). A thick sheath builds up around a small anode, and the sheath edge (plasma side) can be thought of as a large collector of electrons from the positive column.

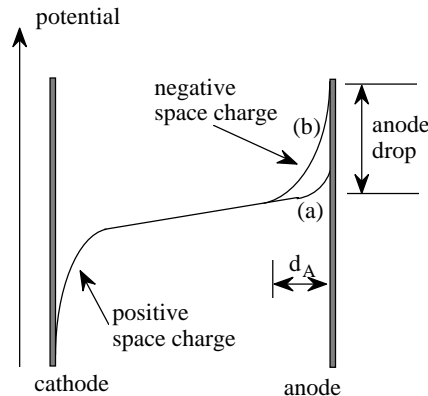


Fig. 8 Potential distribution of an ordinary glow discharge (a) and a hollow-anode discharge (b). Anode drop and sheath thickness, d_A , are drawn for the hollow-anode discharge, case (b).

At a voltage drop of only 15 Volts, electrons gain just enough energy to ionize a gas molecule; the ionization cross section increases until it reaches a maximum at about 100 eV (Fig. 9). Without anode barrier, no substantial ionization happens in the anode sheath because the electron energy is too low. Considering the mean free path of electrons with velocity v_e in a weakly ionized gas,

$$\lambda_e(v_e) = [n_g \sigma(v_e)]^{-1} = \frac{kT_g}{p \sigma(v_e)} \quad (8)$$

we find that $\lambda_e \approx 20$ mm in the case of 15 eV electrons, i.e. not only the energy is too small to cause substantial ionization but also the anode sheath is collisionless (sheath thickness \ll mean free path). This situation is in contrast when the anode barrier is used: the anode drop increases so that electrons gain higher energy, and simultaneously is the ionization cross section increased leading to a mean free-path of $\lambda_e \approx 4$ mm which is equal to or smaller than the observed sheath thickness (see Fig. 3). Note that the free paths, x , are not grouped about a mean value but their distribution is proportional to $\exp(-x/\lambda)$, and therefore most electrons have a free path smaller than the mean free path, λ [8]. Introducing the anode barrier changes the character of the anode sheath from thin, collisionless to thick, collisional. Both the increase in electron-collecting area and increased plasma density near the anode helps to maintain the current balance at the anode surface.

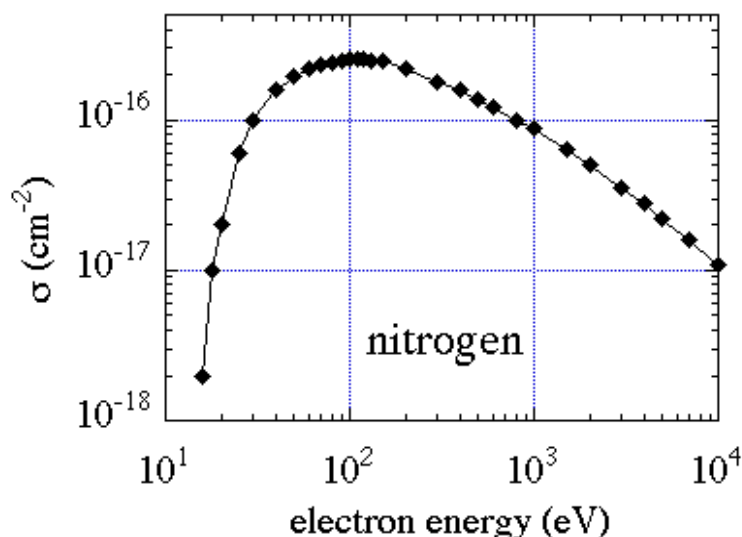


Fig. 9 Cross section of collisional ionization of nitrogen molecules by electron impact (data from [10]).

The results of our experiments indicate it is more precise to speak of a “small-anode discharge” than a “hollow-anode discharge” since the small area and not the hollow geometry is responsible for the observed ionization effects. However, using the “small-anode discharge” in a downstream source requires an opening, and therefore the small anode with a hole is indeed a hollow anode.

Summarizing, we have verified experimentally that the predicted increase of the anode drop is responsible for the existence of a bright anode plasma in a hollow-anode discharge. The increase in the anode potential drop and anode sheath thickness is the response of a glow discharge to a drastically reduced anode area in order to maintain the current balance at the anode surface. This effect can be the basis for a variety of downstream hollow-anode plasma sources, or ion and electron beam sources. We have successfully grown GaN thin films on sapphire using a hollow anode plasma source, and we plan to report about it separately.

Acknowledgments

We are grateful for support and discussions with Michael Rubin, Ian Brown and Michael Dickinson. This work was supported by the U.S. Department of Energy, Division of Advanced Energy Projects, under contract No. DE-AC03-76SF00098.

References

- [1] Miljevic V I, 1984, *Appl. Optics* **23**, 1598
- [2] Miljevic V I, 1984, *Rev. Sci. Instrum.* **55**, 931
- [3] Miljevic V I, 1986, *J. Appl. Phys.* **59**, 676
- [4] Miljevic V I, 1986, *J. Appl. Phys.* **60**, 4109
- [5] Ullrich S, 1976, *Plasma Physics Basics and Methods of Applications of Plasma Probes in Space* (in German), (Berlin: Akademie-Verlag)
- [6] Langmuir I and Mott-Smith H M, 1924, *Gen. Elec. Rev.* **27**, 449, 538, 616, 762, 810; see also: Suits C G and Way H E (Editors), 1961, *The Collected Works of Irving Langmuir*, vol. 4, (New York: Pergamon Press)
- [7] Francis G, 1956, *The Glow Discharge at Low Pressure*, in: *Handbuch der Physik*, ed. by S. Flügge (Berlin: Springer)
- [8] Cobine J D, 1958, *Gaseous Conductors*, (New York: Dover)
- [9] von Engel A, 1994, *Ionized Gases*, (New York: AIP Press), see also: Brown S C, 1994, *Basic Data of Plasma Physics*, (New York: AIP Press).
- [10] Tawara H, Kato T, Ohnishi M, 1985, *Ionization Cross Sections of Atoms and Ions*, Reprint IPPJ-AM-37, Nagoya Institute of Plasma Physics, Nagoya, Japan.